Ain Shams Engineering Journal 12 (2021) 1995–2007

Contents lists available at ScienceDirect

Ain Shams Engineering Journal

journal homepage: www.sciencedirect.com

Mechanical Engineering

Watertight integrity of underwater robotic vehicles by self-healing mechanism

Gang Ma [a], Muhammad Hanis Kamaruddin [a], Hooi-Siang Kang [b,*], Pei-Sean Goh [c], Moo-Hyun Kim [d], Kee-Quen Lee [e], Cheng-Yee Ng [f]

[a] College of Shipbuilding Engineering, Harbin Engineering University, Harbin, Heilongjiang, People's Republic of China
[b] Marine Technology Centre, Faculty of Engineering, Universiti Teknologi Malaysia, 81310 Johor Bahru, Malaysia
[c] Advanced Membrane Technology Research Centre, Faculty of Engineering, Universiti Teknologi Malaysia, 81310 Johor Bahru, Malaysia
[d] Department of Ocean Engineering, Texas A&M University, College Station 77843, TX, USA
[e] Malaysia-Japan International Institute of Technology, Universiti Teknologi Malaysia, Jalan Sultan Yahya Petra, 54100 Kuala Lumpur, Malaysia
[f] Department of Civil and Environmental Engineering, Universiti Teknologi PETRONAS, Perak 32610, Malaysia

ARTICLE INFO

Article history:
Received 18 April 2020
Revised 14 September 2020
Accepted 15 September 2020
Available online 9 December 2020

Keywords:
Underwater robotic vehicle
Self-healing mechanism
Water-tightness
Buoyancy recovery
Damaged stability
Superabsorbent polymer

ABSTRACT

Self-healing mechanism (SHM) application has attracted interest due to ability to self-heal as response to damage situations in various conditions, and is being actively explored. However, the application of SHM that can be autonomously triggered for temporarily keeping structural integrity of underwater robotic vehicle (URV) under flooding condition is still scarce publicly. This paper describes an investigation in watertight integrity performance of URV's hull under damaged stability criteria. The main goal is to investigate the characterization of a rapid SHM through an experiment for identifying progressive flooding in a damaged URV's hull. Here, it is demonstrated that the effectiveness of sodium polyacrylate, a kind of superabsorbent polymers (SAP), had been studied by applying the polymer on an experimental model of damaged URV's hull. A comparison is studied for the stability of the flooded URV and the mass of water accumulated inside the URV's hull between the cases of before and after applying the SHM in the damaged model under different damaged conditions. The results showed that the SHM application had rapidly blocked the damaged leak hole and prevented severe water flow ingress in the damaged URV's hull. Swift recovery of buoyancy was obtained, as the volume of absorbed water by SHM was converted into equivalent buoyancy loss. These findings are establishing a fundamental knowledge for implementation of SHM in underwater robotic structures.

1. Introduction

Many underwater robotic vehicle (URV) are deployed in the coastal and offshore areas to conduct multiple activities, such as oceanography surveillances, underwater operations, and site monitoring. In most of the circumstances, operations in the shallow-water area is associated with strong and intermittent wave surge which requires URV can ride out the wave surge and then repositioning and re-acquiring the objects being sensed. The hull structural integrity of an URV is important to ensure its survivability, especially maintaining the buoyancy and preventing water from damaging the inner electronic sensors and components. The cases of losing underwater robots during operations, such as *Kaiko* [1] and *Nereus* [2] had caused significant properties loss and operational delay to the operators. For structures working in offshore environment, the potential damages of submerged hull are consisting of three categories. The first factor may be attributed to corrosion and fatigue cracking due to age-related damages [3]. Secondly, when combined with transverse bulkhead failure, the impact load from ships and in addition to the external loads can lead to loss of reserve buoyancy [4–6]. The third one is loss of stability, which the

* Corresponding author.
E-mail addresses: magang@hrbeu.edu.cn (G. Ma), hanis.kamaruddin@hrbeu.edu.cn (M.H. Kamaruddin), kanghs@utm.my (H.-S. Kang), gpsean@utm.my (P.-S. Goh), m-kim3@tamu.edu (M.-H. Kim), lkquen@utm.my (K.-Q. Lee), chengyee.ng@utp.edu.my (C.-Y. Ng).
Peer review under responsibility of Ain Shams University.

Production and hosting by Elsevier

https://doi.org/10.1016/j.asej.2020.09.019
2090-4479/

Nomenclature

$C_5H_7NaO_3$	Methyl acetoacetate, monosodium salt	S_B	Wetted body surface
g	Gravitational acceleration (m s^{-2})	S_A	Water surface cut out by wetted body surface
M	Mass (kg)	V_{ao}	Volume of air in an intact URV's hull
P	Pressure (kg m^{-1} s^{-2})	V_{wi}	Volume of water ingress
T	Temperature (°C)	B_o	Intact buoyancy force
ρ	Density of the fluid (kg m^{-3})	B_N	Buoyancy force for a column hull without a self-healing mechanism
V	Submerged volume (m^3)	B_{SH}	Buoyancy force for a column hull with a self-healing mechanism
F	Constraining force from external support	R_B	Recovery buoyancy force
Φ	Velocity potential		
I	Moment of Inertia		

result of hold flooding [7–9]. Once there is an opening of leakage under the sea level, the damaged hull compartments will be fully flooded. The increase of total payload inside the hull by inflow water, will affect the stability and centre of gravity of the damaged hull from their original condition [10]. The change of hydrostatic pressure due to descent of hull position caused by loss of buoyancy leads to more water flowing into the damaged compartments until the pressure inside the hull is in equilibrium with the inlet pressure [11].

Loss of buoyancy over the design life due to partial or complete flooding of the URV lead to equipment failure, especially on the emergency surfacing system [12], and image detection system [13]. Due to the risks as above, a URV with single column hull, as shown in Fig. 1, may experience malfunction of its internal electronic sensors and components under flooded condition, which can lead to the destroy of the URV [14]. As one of the most critical components in the URV, the water-tightness protection of the onboard electronic module must be monitored throughout all phases. Several aspects need to be specifically considered in designing the URV's hull, such as impact conditions and structural integrity for additions and tapings [15]. Subsequently, the water-tightness of the URV's hull is designed to be similar to the function of ship and submarine hull [16], as the internal compartment is designed to be single column hull. If the compartment is fully flooded due to leakage, the total loss of buoyancy will cause the offshore vehicles, such as URV cannot be recovered [9].

In line with the development of advanced materials, advanced polymer materials are used widely in various applications, such as manufacturing vehicles and daily goods, as well as in engineering applications, including self-healing technology. The idea of self-healing technology of some synthetic polymeric materials comes from the ability of biological systems to perform autonomic healing response upon damages that occur towards the system [17,18]. Conceptually, self-healing material (SHM) have the built-in capability to substantially recover their mechanical properties after damage [19]. Hence, thorough studies and advancement of these polymer materials have been conducted by mimicking the self-healing capability of biological systems.

These materials are anticipated to be used widely attributable to their safety and resilience without distress due to prolonged monitoring and to avoid any external repair. Polymeric materials that can intrinsically heal at damage sites under wet or moist conditions are urgently needed for biomedical and environmental applications [20–22]. Like alternative methodologies that use autotrophs of microalgae, SHM remains resilient to highly concentrated organic wastewater's toxic contaminants by adsorption utilizing ion salts [23–25]. Despite recent progress in the design of self-mending polymeric materials based on crack-activated crosslinking, light, heat or other external stimuli, these remain less than perfectly healed, and, in the case of polymers in wet environments, self-healing technologies are even more limited than those engineered for dry conditions.

Due to such limitations, a composite based SHM is proposed in this paper, by the use of a superabsorbent polymer (SAP) pre-stored in the space between the outer and inner wall of URV's hull. SAP material can absorb and retain a large amount of water and aqueous solutions [26]. One of the most commonly used SAPs in the world is sodium polyacrylate [27]. It is a type of salt made from negatively charged polyacrylate that comes from the carboxylic group, and sodium that neutralizes the polyacrylic acid. Presence of carboxylic group aids water absorption process, and the crosslinking between the polymer chains holds polymers together and averts solubilisation of SAPs in water [28]. The amount of water uptake in this material is strongly reliant on both the salt

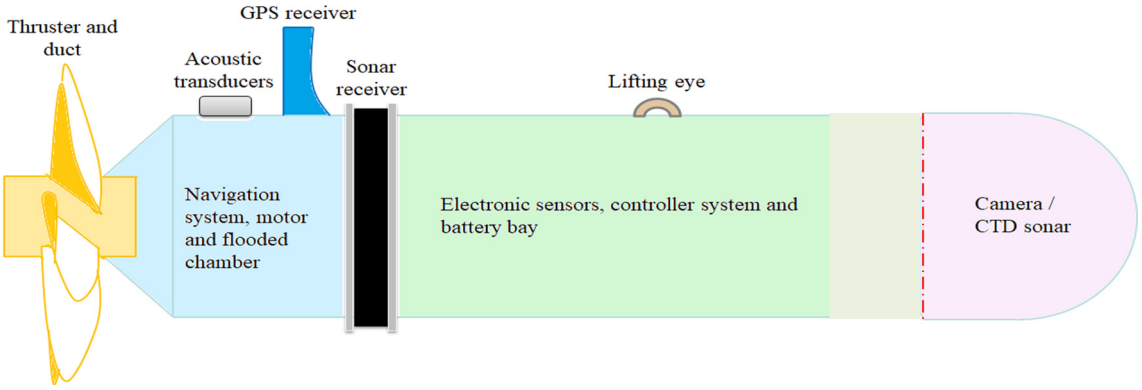

Fig. 1. Typical underwater robotic vehicle (URV) concept.

concentration of the aqueous media and the crosslinking density of the polymers [29]. Therefore, sodium polyacrylate is a highly potential material to ensure water-tightness of the leak-hole on the URV's hull.

The main objective of this study is providing an idea of the time response of URV by varying the buoyancy force, with the existence of hydrostatic pressure phenomenon, as the location of failure between URV vary. To fulfil this objective, the parametric study had been conducted in order to discover the interference effect of the sensitivity of different leak-hole locations, due to hydrostatic pressure phenomena, to the responses of hydrodynamic stability of the damaged URV. This research was extended on the SHM application at selective damage URV configuration in order to make the comparison with damage URV condition. The overall procedures and steps taken in conducting this research are summarized in Fig. 2.

The novelty of studying SHM for the URV is two-fold: firstly, it provides a fundamental understanding on the SHM implementation in underwater robotic hull to prevent further water ingress due to structural leakages; secondly, it can be utilized to specifically assess the effectiveness of SAP experimentally in calm water condition so that its behaviour with regards to water absorption property and the resulting water-tightness effect can be determined. The paper is organized as follows:

Section 2 outlines the different case matrices used to conduct the flooding test of URV's hull model, such as different of leak-hole size and locations, and the SHM application setup. The mathematical modelling of buoyancy force and the physical effects that the models aim to describe. Section 3 presents the outcomes on water tightness condition and the sensitivity of damaged URV without SHM application. The percentage of buoyancy loss caused by the ingress of water into the column hull model with respect to the position of the leak-hole was observed, and the results was used as a basis to SHM application later. Section 4 reveals the findings on SHM application towards the damaged URV. The morphology of SAP before and after swelling was examined, in order to study the effectiveness of SAP characteristic. Section 5 presents a discussion and the SHM can now be predicted by the characterized new buoyancy which generated by empirical formula, and then conclusions are drawn in Section 6.

2. Problem formulation and experimental setup

At zeroth order, an Archimedes' law was derived from conservation of linear momentum as described in Eq. (1):

$$Mg = \rho g V^{(0)} + \mathrm{F}_3^{(0)} \tag{1}$$

Let M be the mass of the entire floating body, part of which may be above the free surface, and $A^{(0)}$ be the area of $S_3^{(0)}$ and

$$I_1^A = \iint_{S_A^{(0)}} (x - X^{(0)})dxdy, \quad I_2^A = \iint_{S_A^{(0)}} (y - Y^{(0)})dxdy \tag{2}$$

be the moments of inertia of the cut plane $S_A^{(0)}$ as derived in Eq. (2) [30], then the linearized z momentum equation at $O(\varepsilon)$ is described in Eq. (3):

$$M[Z_{tt}^{(1)} + \alpha_{tt}\left(\bar{y}^c - Y^{(0)}\right) - \beta_{tt}\left(\bar{x}^c - X^{(0)}\right) = -\rho \iint_{S_B^{(0)}} \Phi_t^{(1)} n_3 dS + \mathrm{F}_3^{(1)} - \rho g(I_2^A \alpha - I_1^A \beta + Z^{(1)} A^{(0)}) \tag{3}$$

If the floating body is totally immersed, $S_A^{(0)}$ vanishes and buoyancy does not affect the dynamic equilibrium.

The buoyancy loss, β of a single cylindrical-based URV's hull is defined by reduction of its intact buoyancy force, $\mathrm{B_o}$ due to water ingress. New buoyancy force, $\mathrm{B_N}$ of a hull after it is reclaimed into a new equilibrium state, is defined in Eq. (4):

$$B_N = B_o - \beta = \rho_w g(V_{ao} - V_{wi}) = \rho_w g \frac{\pi \delta^2}{4}(L - h_w) = (\Delta - \mu)g \tag{4}$$

where ρ_w is density of water, g is gravitational acceleration, V_{ao} and V_{wi} refer to the volume of air in an intact URV's hull and the volume of water ingress, respectively, δ is inner diameter of the URV's hull, L is length of the hull, h_w is height of water ingress in the hull, Δ is displacement of the hull, and μ is mass of water ingress inside the hull.

The experiment was conducted at Marine Technology Centre at Universiti Teknologi Malaysia. A calm water basin with length of 1.00 m, width of 0.45 m and depth of 0.45 m had been utilized to conduct the experiment of buoyancy loss. Fig. 3 shows the layout of the experiment. The single hull model (column) was sub-

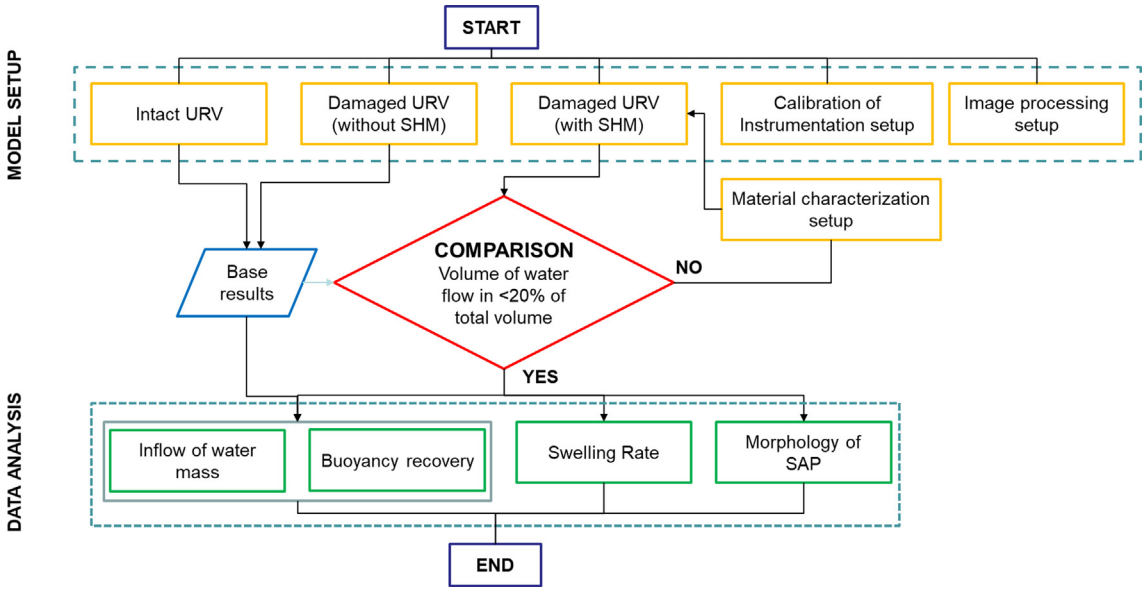

Fig. 2. Research methodology flowchart.

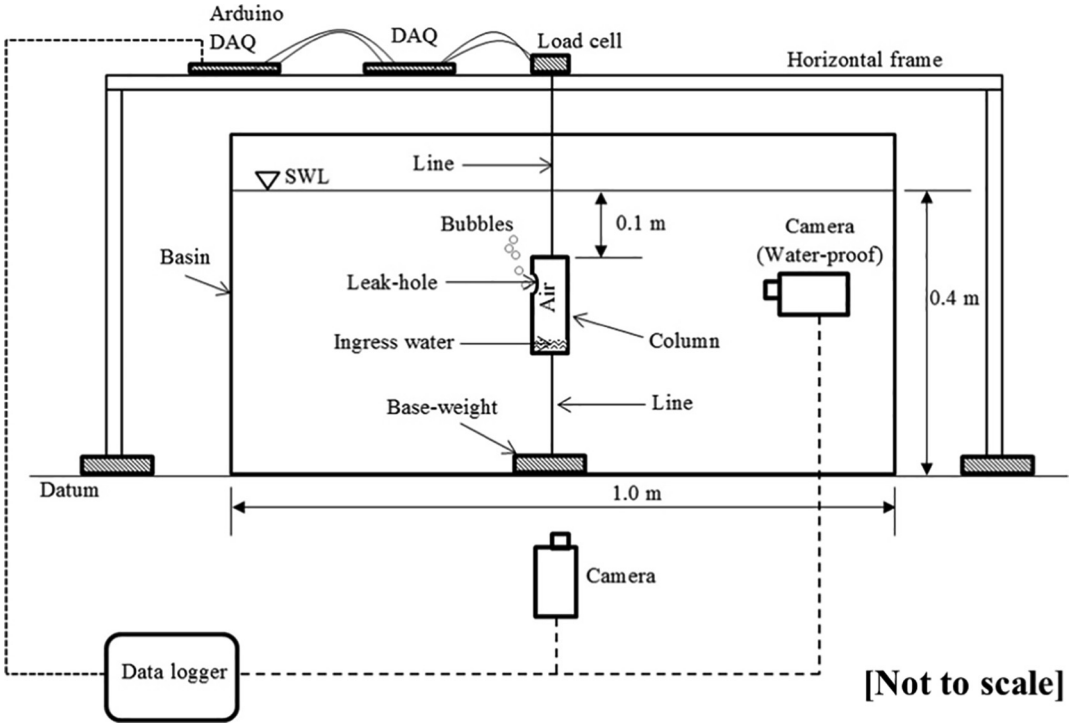

Fig. 3. Schematic diagram of the Flooding Test of URV's Hull.

merged 0.1 m from still-water level to avoid free-surface effects upon the response of the hull model. The single hull model was floated vertically in the water domain in the basin, by mooring it to a base-weight which was located on the bottom floor of the water basin. The test basin was fabricated from transparent acrylic plates for hosting water up to 0.4 m in height. In order to observe the process of water ingress, the model of hull was constructed in the form of transparent prospect acrylic cylinder, which was excellent for visual underwater exploration, and because of its longevity in seawater due to corrosion resistant [31]. The size of single hull model is according to the scale model of the hull of offshore structure; modified based on the works of [32], with a scale of 1:36.67 and slenderness ratio of 3.5 as tabulated in Table 1. A horizontal frame was installed on the top of test basin, where a load cell was attached on the frame and connected to the top of underwater cylindrical hull model, by initially setting the connection line was in zero tension condition. Load cell was operated to measure the in-line tension and tension variations of the hull with respect to buoyancy loss during the experiment runs. These values were then converted into total buoyancy loss. Portable data acquisition system consisting of HX711 amplifier board and Arduino board was utilized to record the signals from the load cell. Two cameras were utilized to record the mechanism of water ingress and self-healing mechanism of the hull model from the front view and the underwater view. The videos recorded by the cameras were then converted into a sequence of still images to determine the effectiveness of water ingress generated with- and without the self-healing mechanism.

Table 1
Principal parameters of the underwater single column hull model.

Parameters	Dimensions
Outer diameter, D (mm)	36.0
Inner diameter, δ (mm)	32.5
Length, L (mm)	126.0
Displacement, Δ (kg)	0.104
Mass, $\boldsymbol{m}$ (kg)	0.060
Slenderness ratio, a^*	3.5

Note: Slenderness ratio, $a^* = L/D$.

2.1. Case matrices

As shown in Figs. 4, 5 and Table 2, the experiment for an underwater column hull model of URV was conducted for five different cases, which were Case I – leak-hole at different locations, Case II –leak-holes with different size, Case III – effects of top and bottom holes, Case IV - side leak-holes at different locations with SAP layer as self-healing mechanism, and Case V – top leak-hole with SAP layer with different thickness. In general, the first three cases were referred to as a setting of URV's hull model without self-healing mechanism.

2.1.1. Flooding test of URV's hull model without SHM

In Case I, a leak-hole of a round shaped with diameter of 1/3 D (where D is an outer diameter of the column hull model) was set with lengths of 0.127 L, 0.365 L, and 0.603 L (where L is a length of the column hull model), respectively, from the bottom of the model. The sensitivity of leak-hole location, h for inflow of water mass, μ was then studied. On the other hand, different locations of 0.127 L, 0.365 L, and 0.603 L were determined based on certain limited states. Leak-holes might be due to collision, corrosion or fatigue failures. In Case II, three different leak-hole sizes of 1/6 D, 1/4 D, and 1/3 D had been investigated. Later in Case III, the amount of inflow of water mass was determined when the leak-hole was set at top or the bottom of an underwater column hull model. The distance from the centre of the leak-hole to the centre of the underwater column hull model was 0.22 D in Case III.

2.1.2. Flooding test of URV's hull model with SHM in the hull structure

Case IV and Case V cater for an underwater column hull model of the URV with self-healing mechanism. In both cases, the hull

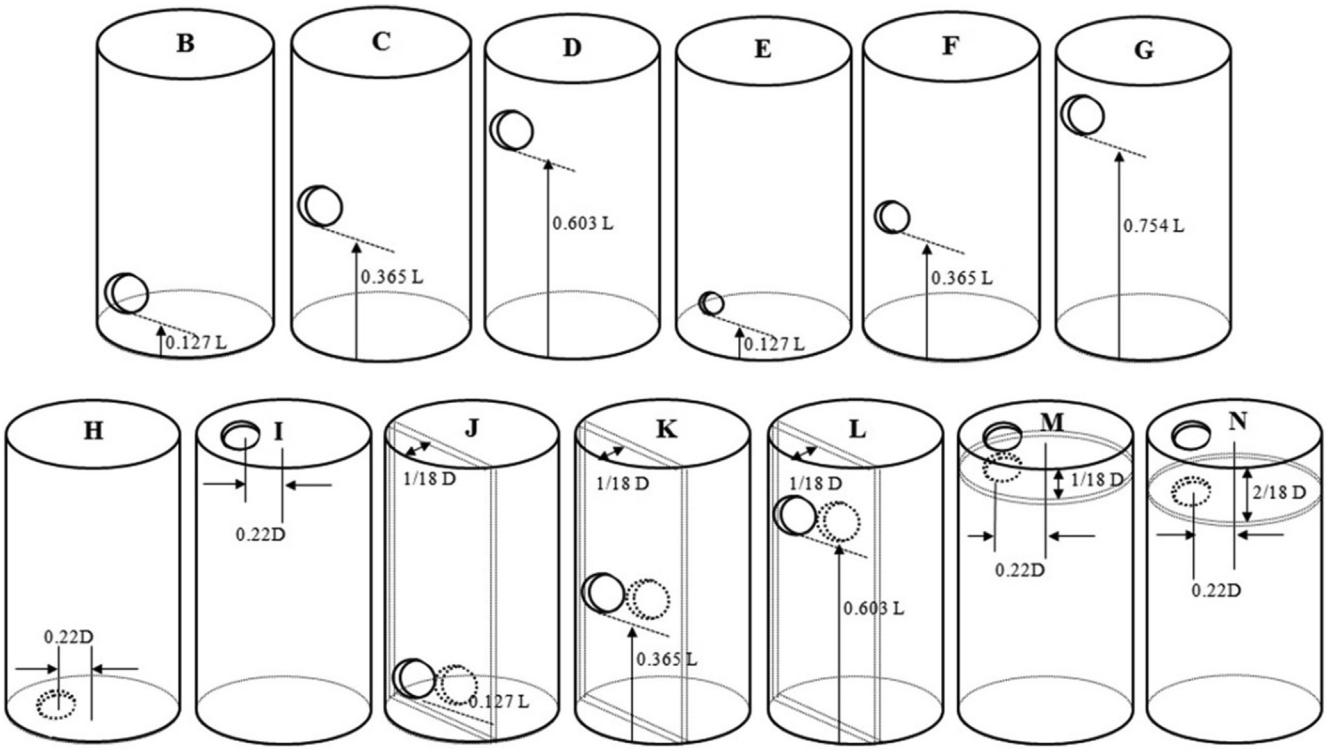

Fig. 4. Leak-holes arrangement of damaged underwater column hull model for (a) Case I – different locations of leak-holes (B–D), (b) Case II – different sizes of leak-holes (E–G), (c) Case III – leak-holes at the top and the bottom (H and I), (d) Case IV – side leak-holes at different locations with SAP layer (J–L), and (e) Case V – top leak-hole with SAP layer with different thickness (M and N).

structure of the column model was modified to include a self-healing mechanism as a composite layer. An inner wall, which was made of prospect acrylic plate, was added in the column hull model. The leak-holes were fabricated on the inner wall accordingly to form a channel for air/water exchange.

A superabsorbent polymer (SAP), which has hydrophilic properties and is able to expand in volume, was filled into the space in between the outer wall and inner wall of the modified hull structure, as shown in Fig. 5. In order to observe the process of water ingress, the composite layer of the underwater column hull model was constructed from a transparent prospect acrylic. The combined layers across the hull wall were located at the right angle of observation so that the changes of self-healing mechanism could be recorded. A kind of advanced polymer materials, sodium polyacrylate, was chosen as the SAP material in this research. The properties of sodium polyacrylate are shown in Table 3. In Case IV, SAP layer with thickness of 1/18 D was added as the self-healing composite layer, whereas in Case V, two different thicknesses of SAP layer, which were 1/18 D and 1/9 D, respectively, had been studied. It was expected that the new buoyancy for a column hull with a self-healing mechanism, B_{SH} should be larger than the one without a self-healing mechanism B_N. The recovery buoyancy, R_B is defined in Eq. (5) as:

$$R_B = B_N - B_{SH} \tag{5}$$

3. Water-tightness condition without SHM

3.1. Sensitivity of location of leak-hole

The results for the underwater column hull model without self-healing mechanism are presented in Fig. 6 and Table 4. For Case I and Case III, it was found that the new equilibrium of water level of the inflow of water mass into the column model depended on the height of the leak-hole.

Table 4 shows the flow of water into the underwater column hull model under conditions of B, C, D, G, and I. Water stopped flowing into the column hull model when the pressure of the remaining air entrapped inside the model was in equilibrium with the pressure of water at the leak hole [33]. On the other hand, the water did not flow in under condition H, in which the leak hole was located on the bottom of the model. The percentage of buoyancy loss caused by the ingress of water into the column hull model with respect to the position of the leak-hole was observed in both Cases I and III. The losses of buoyancy under conditions H, B, C, D, and I (from the bottom to the top of the column hull model) were 0.0%, 21.2%, 45.2%, 70.2%, and 100.0%, respectively, as shown in Fig. 7. It is noteworthy that in this experiment, the submerged position of the damaged column hull model in the calm water was kept vertical due to the absence of wave and current. The existence of wave and current could have caused further inclination of the column hull model, hence allowing the entrapped air volume inside the column to be further discharged. Meanwhile for I condition, since the density of air is lighter than water, it makes the air become easier to release out, hence the water starts to fill in until the damaged URV is totally submerged. The higher location of the leak-hole required a longer duration for the water level to reclaim its new equilibrium state [34]. The time to reach a new equilibrium state under conditions H, B, C, D, and I were 0 s, 3 s, 5 s, 9 s, and 10 s, respectively.

3.2. Sensitivity of size of leak-hole

In Case II Condition E, there was no water flowing into the damaged underwater column hull model when the diameters of leak-hole were 1/6 *D*. A possible reason is the absolute sizes of this leak-hole were too small, thus surface tension of the water around the leak hole [35] had sufficient strength to resist the air/water

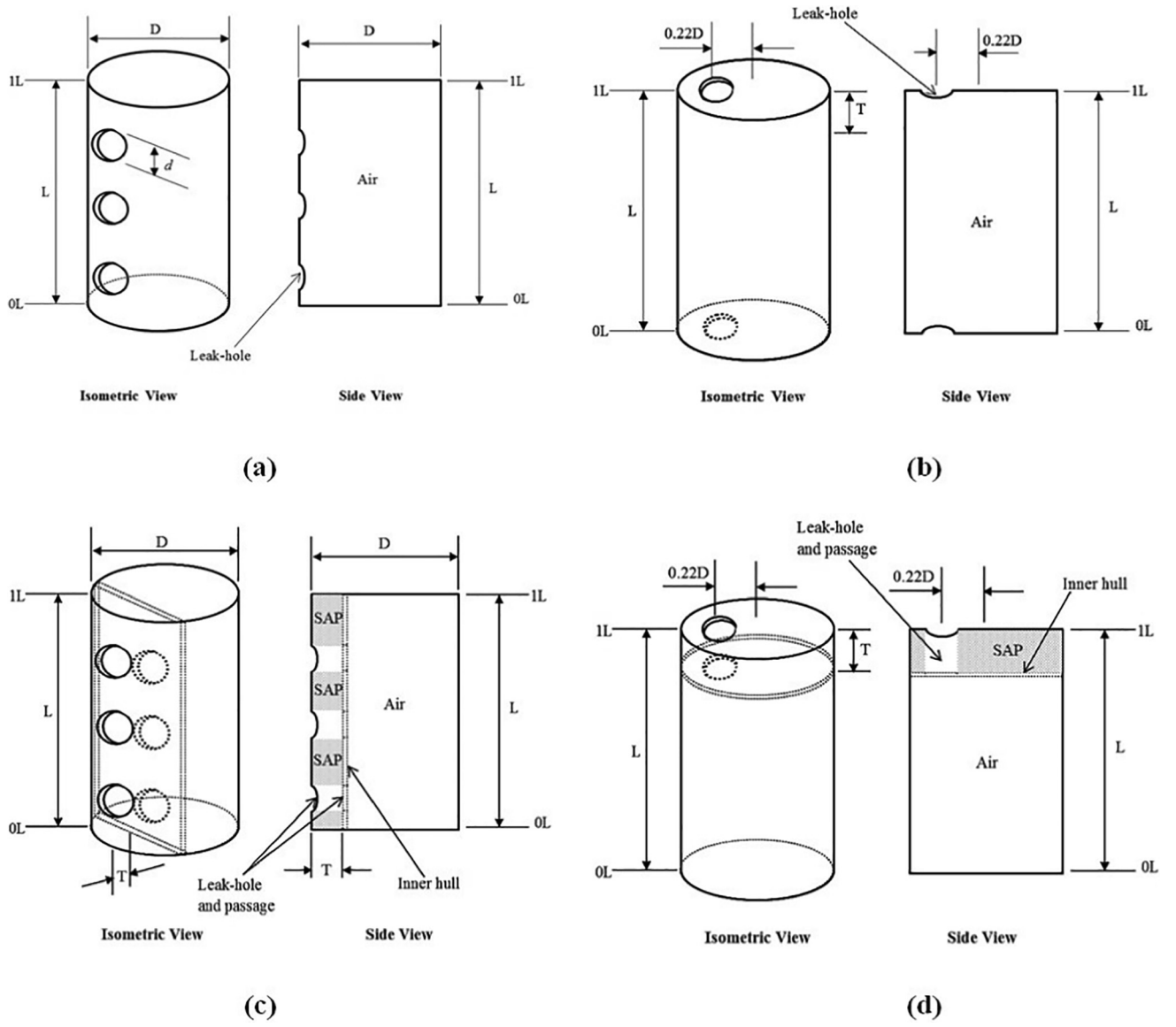

Fig. 5. Structural arrangement of the underwater column hull model for (a) conditions B-G, (b) conditions H and I, (c) conditions J, K, and L, and (d) conditions M and N.

Table 2
Parametric case study of the underwater column hull model.

Case	Condition	Location of leak-hole lowest edge from bottom, *h*	Size of leak-hole, *d*	Thickness of SAP layer, *T*	Mass ratio of SAP/Column (%)
I	B	0.127 L	1/3 D	–	–
	C	0.365 L	1/3 D	–	–
	D	0.603 L	1/3 D	–	–
II	E	0.127 L	1/6 D	–	–
	F	0.365 L	1/4 D	–	–
	G	0.754 L	1/3 D	–	–
III	H	0.000 L	1/3 D	–	–
	I	1.000 L	1/3 D	–	–
IV	J	0.127 L	1/3 D	1/18 D	1.4%
	K	0.365 L	1/3 D	1/18 D	1.4%
	L	0.603 L	1/3 D	1/18 D	1.4%
V	M	1.000 L	1/3 D	1/18 D	0.6%
	N	1.000 L	1/3 D	2/18 D	0.8%

Note: L = length of column hull model; D = outer diameter of column hull model.

exchange. It is apparent from this result that this force is balanced by the pressure difference, Δ_P, between the internal pressure (atmospheric pressure), and the external pressure that acting over the circular area. Since findings of surface tension are mostly based on empirical study, further experimental investigation is highly required in future works.

Table 3
Properties of sodium polyacrylate.

Form	Powder (Free-flowing granular)
Crosslinking	Cross-linked
Particle Size	90–850 m
Density	0.54 g/mL at 25 °C
Formula	$C_5H_7NaO_3$
Formula weight	94.04 g/mol

4. Water-tightness condition after incorporation of SHM

As previously mentioned in Introduction section, the application of SHM in wet environment is still less in number. Henceforth, the study of the effect of SAP on the amount of water inflow into damaged URV was observed through the experiment conducted. The results of an underwater column hull model with self-healing mechanism are presented in Fig. 8 and Table 5. For both Cases IV and V, the self-healing composite layer could significantly stop the ingress of water into the column hull model. The process of water absorption by SAP was stopped when this material became partly swollen. The swollen sodium polyacrylate blocked the leak-hole, causing water-tightness effect across the leak hole of the damaged underwater column hull. Water stopped flowing into the column hull model when the SAP absorbed a certain amount of the inflow of water and expanded in volume until fully blocking the leak-hole. A new equilibrium state was formed in between the remaining entrapped air inside the column hull model and the pressure of water located just outside the leak hole, where these two fluids were separated again by an aqueous-swellable SAP. The losses of buoyancy under conditions J, K, L, M, and N were 5.8%, 8.7%, 10.6%, 21.2%, and 16.3%, respectively. This is because, the closer hole to the bottom of the damaged URV tends to have higher hydrostatic pressure, and the velocity of water inflow rate

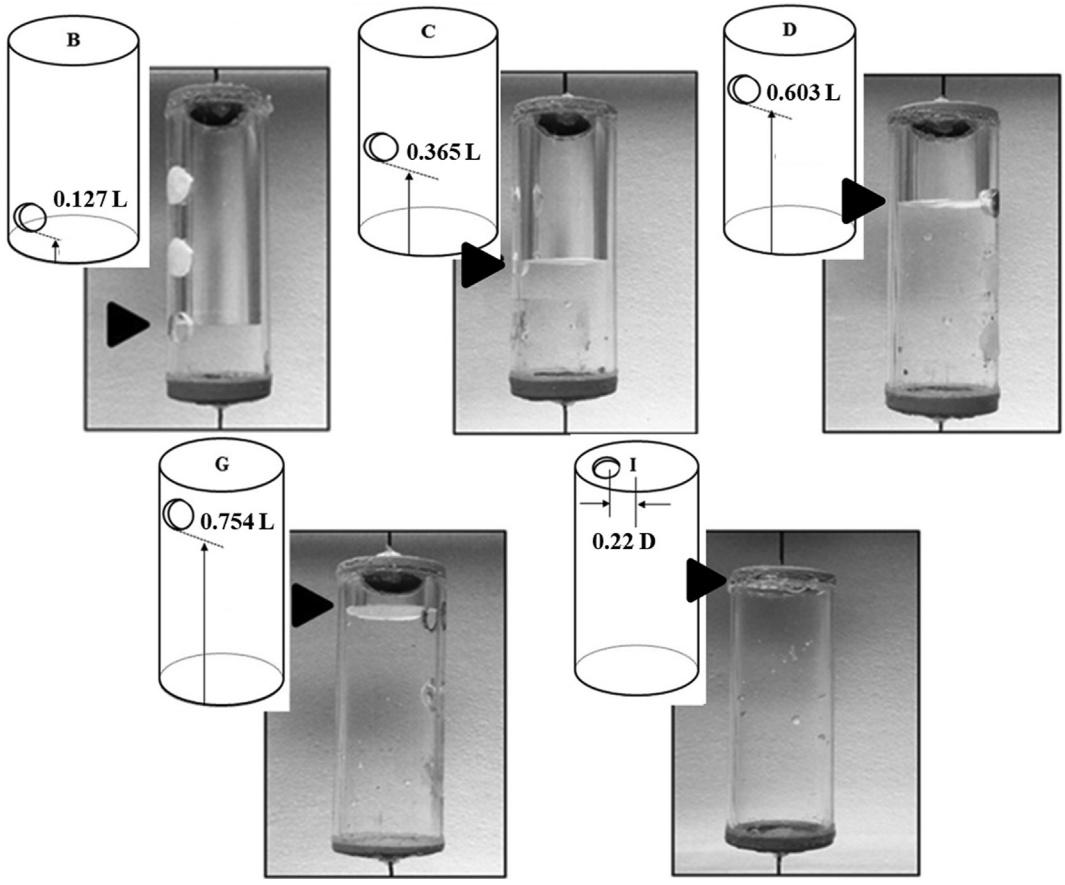

Fig. 6. Underwater view of the flooded compartment of the underwater column hull model without self-healing mechanism in a new equilibrium state.

Table 4
Results of damaged underwater column hull model without self-healing mechanism.

Case	Condition	Inflow of water mass, μ (kg)	Percentage of buoyancy loss, β	Time taken to reach new equilibrium state, t (s)
I	B	0.022	21.2%	3
	C	0.047	45.2%	5
	D	0.073	70.2%	9
II	E	0.000	0.0%	0
	F	0.000	0.0%	0
	G	0.088	84.6%	10
III	H	0.000	0.0%	0
	I	0.104	100%	10

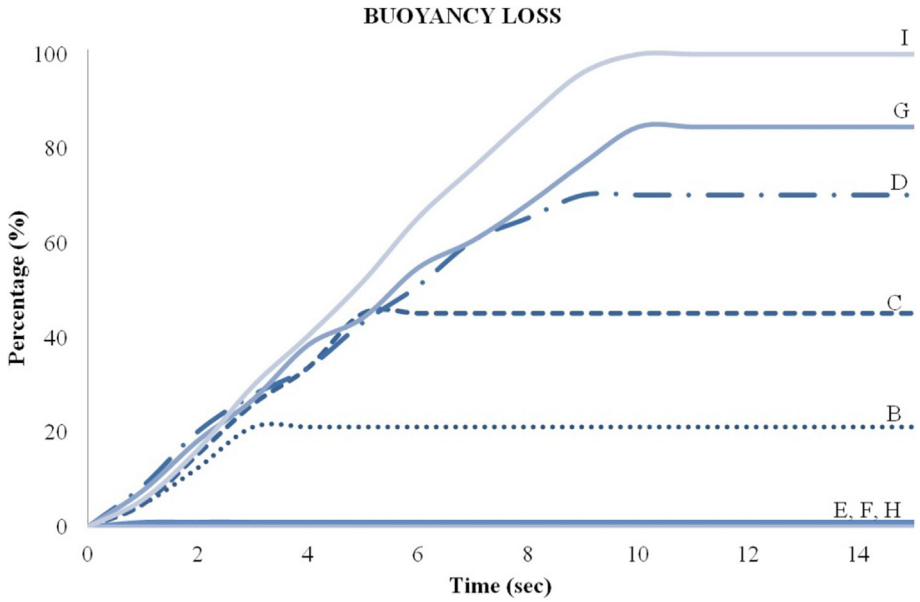

Fig. 7. Percentage of buoyancy loss of the damaged underwater column hull model without self-healing mechanism.

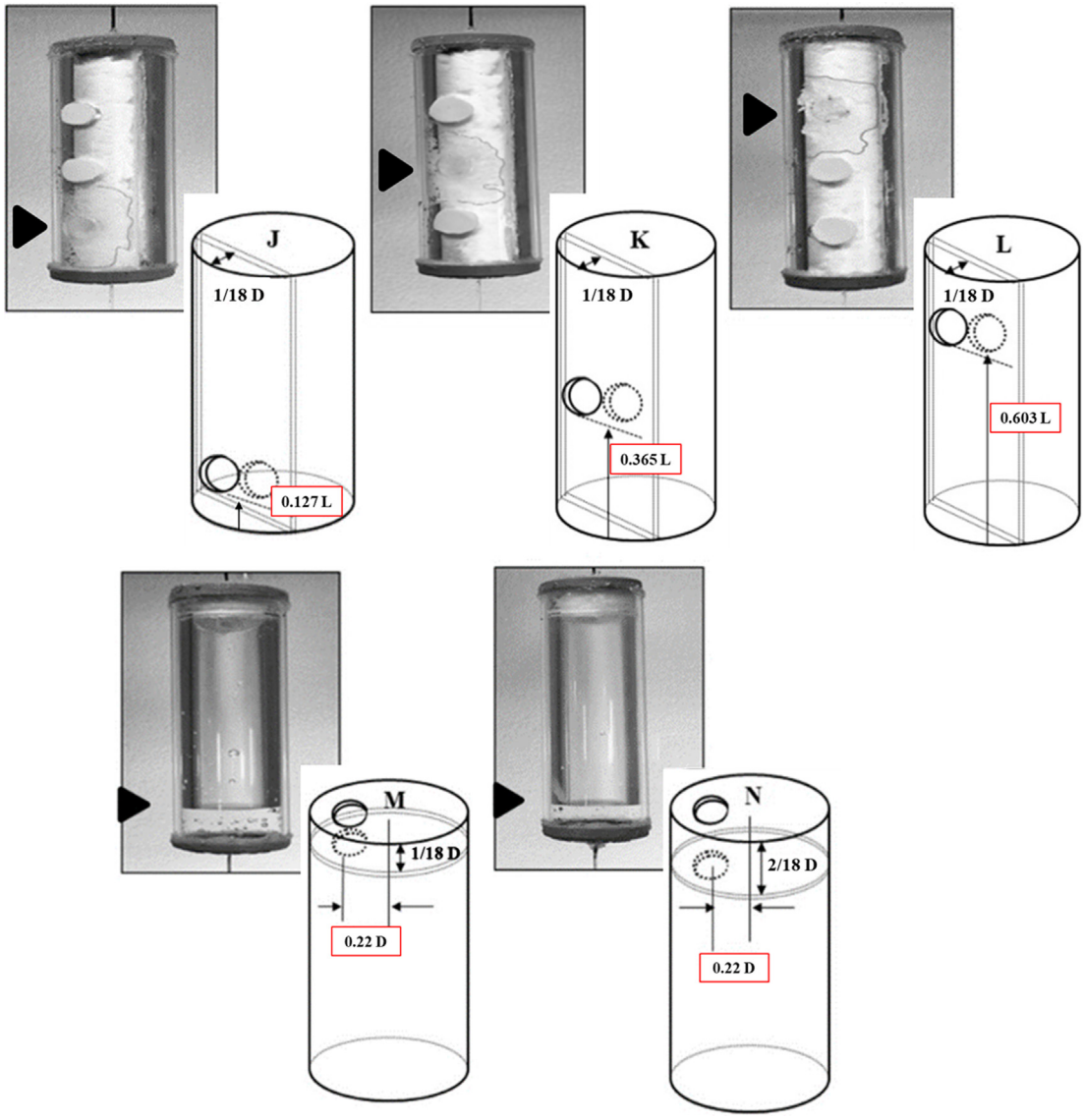

Fig. 8. Underwater view of the flooded compartment of the underwater column hull model with a self-healing mechanism at in new equilibrium state.

Table 5
Results of damaged underwater column model with self-healing mechanism.

Case	Condition	Inflow of water mass, μ (kg)	Percentage of buoyancy loss, β	Time taken to reach new equilibrium state, t (s)
IV	J	0.006	5.8%	<1
	K	0.009	8.7%	<1
	L	0.011	10.6%	<1
V	M	0.022	21.2%	5
	N	0.017	16.3%	6

is slower for J, K and L condition. As the water inflow rate is low, the absorption rate by SAP will become faster, and the damaged hole will be blocked by the swollen SAP. It is noteworthy that in both Cases IV and V, the flooding water had been successfully blocked by the SAP composite layer from flowing across the leak-hole into the inner air compartment. The excellent accomplishment in the SAP implementation can be observed from the big gap difference between I and M/N condition. Both conditions were conducted at the same damaged hole location (at the top of the URV), but the differences are the length of the compartment to occupy the SAP. The damaged URV in condition I is totally submerged because no SAP was implemented. Meanwhile in condition M/N, both conditions only allow a little amount of water to fill in, and managed to block the water entry in a swift response. Besides, the most important part is the damaged URV can maintain their positioning due to the recovery buoyancy.

4.1. Morphology of SAP

To demonstrate the improved properties of the SAP and its suitability for use in marine industry, the morphology of SAP matrix before and after swelling was examined by using scanning electron microscope (SEM). Furthermore, SEM analysis was used to determine the average particle sizes and porous distribution [36]. The porous structure of SAP is shown in from Fig. 9(a) and (b) where irregular pores were distributed across the structure. The porous structure increased the surface area and allowed the absorption of high amounts of liquid. Fig. 9(c) and (d) show the surface morphology of SAP after water absorption. The porous structure was no longer visible in the intercalated structure of SAP. This finding shows a good comparison with Mahon et al.'s research [37], as the SAP was having a wider pore-size distribution and it tends to be more porous structure as shown similarly in Fig. 9(c) and (d). The swelling performance of the SAP could be determined by its pore size distribution.

4.2. Recovery of buoyancy

The time to reach a new equilibrium state under conditions J, K, and L were all less than 1 s, but were 5 s and 6 s under conditions M and N, respectively. Since a certain amount of the inflow of water was absorbed by the SAP to trigger the self-healing mechanism, the total final payload was increased accordingly. After certain volume of absorbed water by SAP had been converted into equivalent buoyancy loss, the recovery percentage of the buoyancy could be obtained. The recovery of buoyancy, R_B, calculated from the difference of condition without self-healing mechanism to a condition with self-healing mechanism, were J/B = 15.4%, K/C = 36.5%, L/D = 59.6%, and M/I = 78.8%, when the thickness of the SAP composite layer was 1/18 D. Again, the underwater posi-

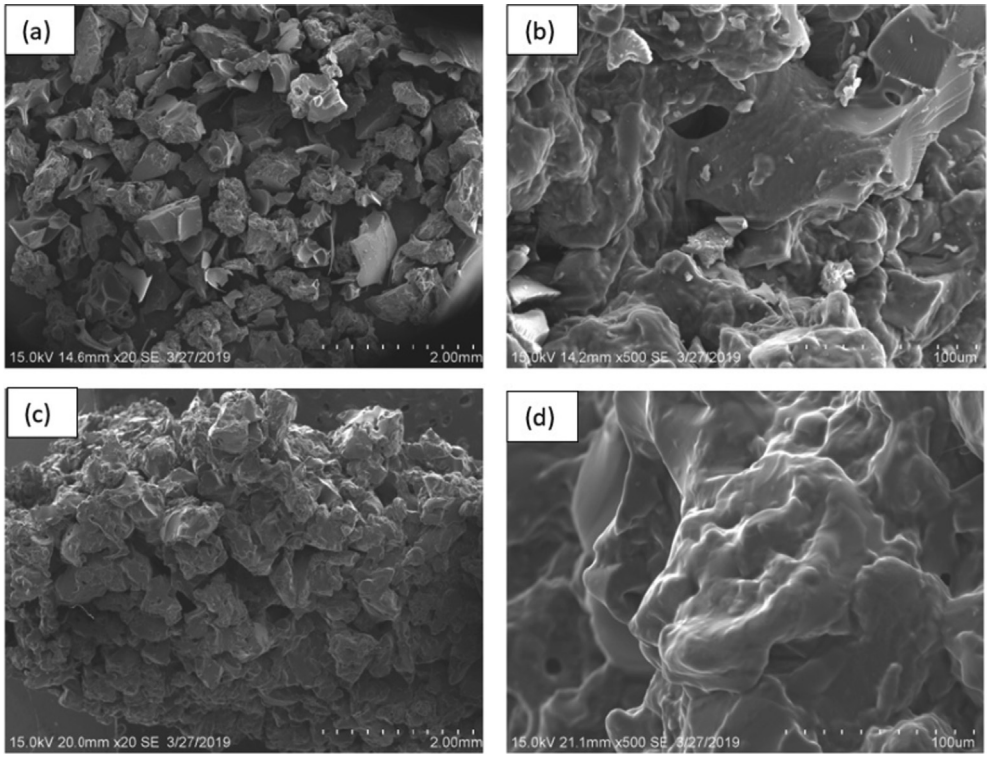

Fig. 9. SEM images of (a, b) SAP and (c, d) SAP after swelling with different magnifications (20× and 500×).

tion of the damaged column hull model was kept vertically in calm water without the presence of wave and current in this experiment.

4.3. Swelling rate

It is interesting to note that the swelling rate of the SAP implied a proportional relationship to the height of the side leak-hole under conditions J, K, and L. Lower position of the side leak hole led to lesser amount of absorbed water by the SAP to fully block the leak hole and reclaim equilibrium state. This finding was consistent with the results of both M and N conditions, where the leak-hole was located at the top of the hull model. A small amount of flooding water was captured inside the air compartment of the underwater column hull model in both M and N conditions before the leak-hole could be fully blocked by the self-healing mechanism of the SAP composite layer.

This phenomenon could be due to the pressure gradient across the hull wall, which varied along with the height of underwater column hull. The inner air pressure inside the air compartment remained identical regardless of the position, whereas the outer hydrostatic pressure varied with respect to the submerged depth [38]. From the results of the experiment, it was found that the air/water exchange rate at the lower part of the column model was gradually lower than the one at the upper part of the column model. Hence, the air on the lower side of the compartment was assumed facing larger resistance to escape through the leak-hole. Since the air/water exchange rate increased from the bottom to the top, as found in this experiment, a bigger volume of the ingress of water flowed in at the upper part of the column hull model and absorbed by the SAP before the passage was fully blocked. A further experimental investigation to study the correlation of a swelling rate of the SAP materials with respect to the leak-hole position is highly required in the future works.

5. Empirical formulation for buoyancy recovery

In general, the self-healing mechanism was able to retain the majority of the underwater column hull model buoyancy by blocking the leak-hole within a very short period (from 1 to 6 s in the experiment). Fig. 10 shows the results of the remaining buoyancy of the damaged underwater column hull models in all experimental cases. The recovery buoyancy of the underwater column hull models with self-healing mechanism (Cases IV and V) was considerably higher than the buoyancy force retained in the damaged column hull model without self-healing mechanism (Case I). On the other hand, for the leak-hole located at the top of the underwater column model (Case V), it was observed that with thicker layer of self-healing SAP composite, the buoyancy recovery from damaged underwater column hull structure was higher. Fig. 11 shows a curve fitting result for the remaining buoyancy force inside the damaged underwater column hull model. By knowing that h was the position of the lowest edge of the leak-hole from the bottom of the column hull model, the characterized new buoyancy for a column hull without self-healing mechanism, B_N and for column hull with a self-healing mechanism, B_{SH} can be defined in Eq. (6) as:

$$\begin{cases} B_N = 40.51h^2 - 139.41h + 98.62 \\ B_{SH} = -15.64h^2 + 0.53h + 94.10 \end{cases} \quad \text{for} \quad 0 \leqslant h \leqslant 1L \tag{6}$$

5.1. Reconsideration of damaged stability with SHM

In general, the characterization of self-healing mechanism can now be predicted by using Eq. (6). It is noteworthy that the B_N curve is generally applicable to a damaged column hull, whereas the B_{SH} curve can be further modified for other types of SAP. Since the size of single column URV is always much smaller than that of conventional underwater submarines, the total allowable buoyancy loss, β during accidental flooding is relatively smaller. Hence, the B_{SH} curve is an important guideline to investigate the damaged stability of the URV, although damaged stability for URV is not compulsory to be investigated since it was unmanned vehicle operated. However, being able to keep it afloat during a damaged condition is a favourable option when the cost to recover a sunk URV is larger, with respect to the exploration depth and the size of URV, which have been increasing rapidly. An upscaling study to determine the application in full scale is needed in future works. A possible challenge in upscaling study is the practicality of SAP,

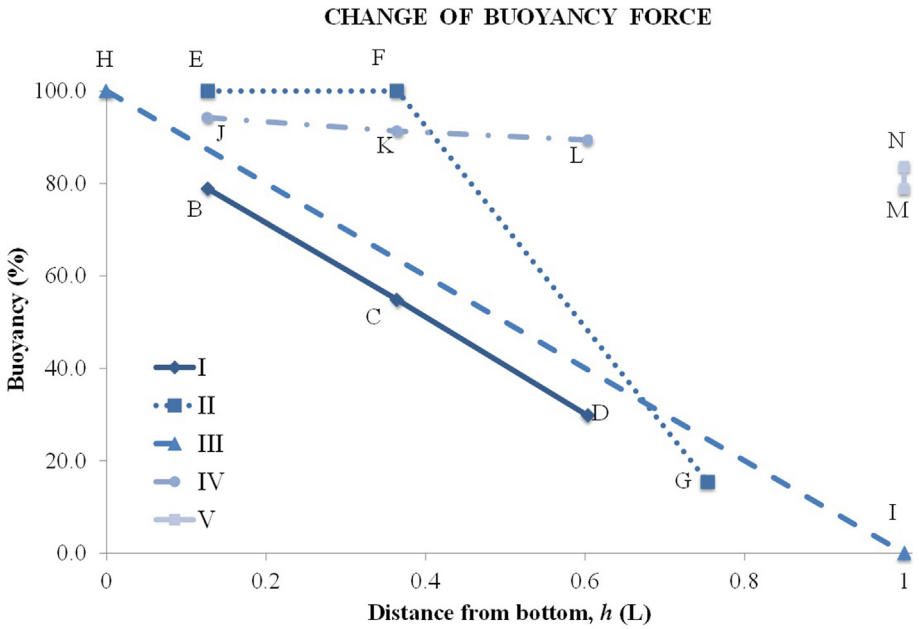

Fig. 10. Changes of buoyancy force according to the location of leak-holes.

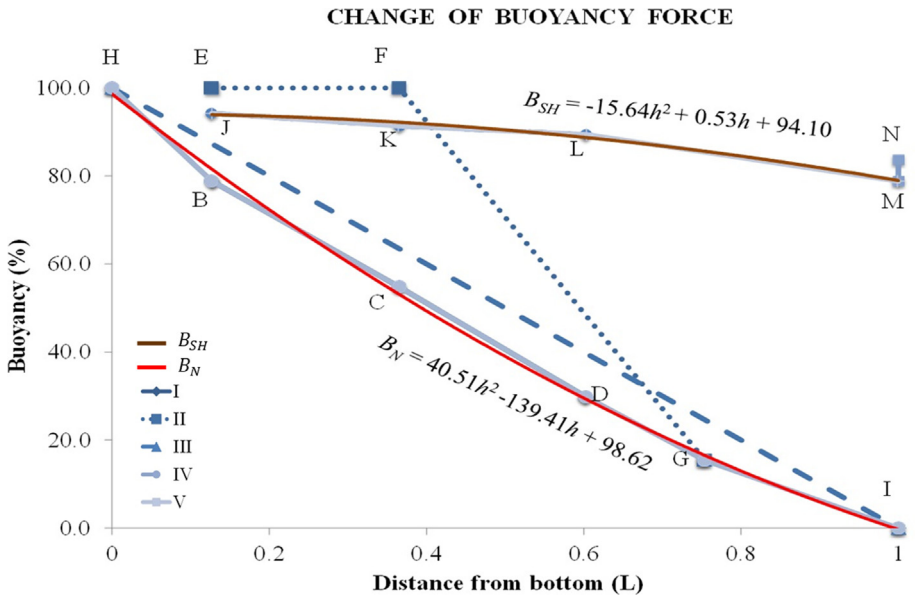

Fig. 11. Buoyancy of damaged underwater column hull model with respect to the location of leak-holes.

thus requires further analysis. The sodium polyacrylate used in this experiment was able to block progressive flooding from the leak-hole by its swellable properties in an aqueous medium. This material may not be the most suitable or only type of SAP practical for implementation in marine environment, hence comprehensive studies on swelling rate, dissolution rate, and strength of cross-link of other types of SAP are recommended. A new material should be able to form a typical B_{SH} curve, regardless of different coefficients, as long as with similar trend as shown in Fig. 11. On the other hand, the selected SAP shall be subjected to a life cycle assessment in order to assess the reliability of the material, material cost, and total production cost. In addition, the material and total production cost incurred with the adaptations of the fabrication system for a full-scale hull with incorporation of SHM layer shall be assessed accordingly.

6. Conclusions

Experimental studies on the effectiveness of self-healing SAP composite layer for underwater column hull model of URV have been carried out. Comparisons between the damaged column hulls, with a self-healing mechanism and without a self-healing mechanism, respectively, have been evaluated through performing buoyancy loss analyses.

As such, these findings from the implementation of self-healing SAP are expected to contribute greatly to the safety and durability to the URV without the high costs of active monitoring. Besides, it could prolong the lifespan of the damaged URV during the salvage operation. The main results are summarized as follows:

- New equilibrium of water level of the inflow of water mass into the column hull model depends on the height of the leak-hole, in which higher location of the leak-hole requires longer duration for the water level to reclaim its new equilibrium state.
- The recovery of buoyancy and swelling rate of the SAP are proportional to the height of the leak-hole, where lower position of the side leak hole means lesser absorbed water by SAP to fully block the leak hole.
- A self-healing mechanism will help to retain majority of the underwater column hull model buoyancy by blocking the leak-hole completely, and eventually stop the water from flowing into the damage area. Consequently, the damaged URV could maintain their stability positioning while the swelling SAP is fully blocked the leak-hole.

The self-healing mechanism in the underwater column hull is promising for the model scale. However, in this study, the recovery of buoyancy and swelling rate of the SAP. To fully evaluate the applicability of the SHM, future works should address more on the effect of URV under complex dynamic behaviour, and more practicality of SAP. Nevertheless, the present study should be useful as it provides a novel concept for further design consideration of URV.

Declaration of Competing Interest

The authors declare that they have no known competing financial interests or personal relationships that could have appeared to influence the work reported in this paper.

Acknowledgements

The authors would like to appreciate the National Natural Science Foundation of China (Grant Nos. 51979050, 51739001, 51979062), the Natural Science Foundation of Heilongjiang Province of China (Grant No. E2017029), the National Key Research and Development Program of China (Grant No. 2017YFE0106400), and Universiti Teknologi Malaysia (GUPCOE Grant No. 03G92) for the supports in preparing this paper. Any opinions, findings and conclusions or recommendations expressed in this publication are those of the authors and do not necessarily reflect the views of the above-mentioned organizations.

References

[1] Momma H, Watanabe M, Hashimoto K, Tashiro S. Loss of the full ocean depth ROV Kaiko - Part 1: ROV Kaiko – a review. In: Proc. Int. Offshore Polar Eng. Conf.; 2004.
[2] Showstack R. Unmanned research vessel lost on deep sea dive. Eos (Washington DC) 2014. doi: https://doi.org/10.1002/2014EO200004.
[3] Vu Van T, Yang P. Effect of corrosion on the ship hull of a double hull very large crude oil carrier. J Mar Sci Appl 2017. doi: https://doi.org/10.1007/s11804-017-1425-7.

[4] Ehlers S, Tabri K, Romanoff J, Varsta P. Numerical and experimental investigation on the collision resistance of the X-core structure. Ships Offshore Struct 2012. doi: https://doi.org/10.1080/17445302.2010.532603.
[5] Ko YG, Kim SJ, Paik JK. Effects of a deformable striking ship's bow on the structural crashworthiness in ship–ship collisions. Ships Offshore Struct 2018. doi: https://doi.org/10.1080/17445302.2018.1442115.
[6] Qasim RM, Hasan AQ. Investigating the behavior of offshore platform to ship impact. Civ Eng J 2020.
[7] Xiang X, Yu C, Zhang Q. On intelligent risk analysis and critical decision of underwater robotic vehicle. Ocean Eng 2017. doi: https://doi.org/10.1016/j.oceaneng.2017.06.020.
[8] Youssef SAM, Noh SH, Paik JK. A new method for assessing the safety of ships damaged by collisions. Ships Offshore Struct 2017. doi: https://doi.org/10.1080/17445302.2017.1285679.
[9] Konovessis D, Chua KH, Vassalos D. Stability of floating offshore structures. Ships Offshore Struct 2014. doi: https://doi.org/10.1080/17445302.2012.747270.
[10] Mohamed SA, Osman AA, Attia SA, Maged SA. Dynamic model and control of an autonomous underwater vehicle. In: 2020 Int. Conf. Innov. Trends Commun. Comput. Eng., IEEE; 2020. p. 182–90. https://doi.org/10.1109/ITCE48509.2020.9047757.
[11] Kim JS, Roh MII, Ham SH. A method for intermediate flooding and sinking simulation of a damaged floater in time domain. J Comput Des Eng 2017. doi: https://doi.org/10.1016/j.jcde.2016.09.005.
[12] Michaud M. Rules for building and classing underwater vehicles, systems and hyperbaric facilities. In: Underw. Interv. Conf. 2009, UI 2009, 2008.
[13] Dai W, Jiang J, Ding G, Liu Z. Development and application of fire video image detection technology in China's road tunnels. Civ Eng J 2019. doi: https://doi.org/10.28991/cej-2019-03091221.
[14] Zhu D, Sun B. Information fusion fault diagnosis method for unmanned underwater vehicle thrusters. IET Electr Syst Transp 2013. doi: https://doi.org/10.1049/iet-est.2012.0052.
[15] Eugene Allmendinger E. Submersible vehicle systems design. Illustrate. Society of Naval Architects and Marine Engineers; 1990.
[16] Jasionowski A, Vassalos D, Guarin L. Time-based survival criteria for passenger Ro-Ro vessels. Fluid Mech Appl 2011. doi: https://doi.org/10.1007/978-94-007-1482-3_38.
[17] Chandra Sekhara Reddy T, Ravitheja A. Macro mechanical properties of self healing concrete with crystalline admixture under different environments. Ain Shams Eng J 2019. doi: https://doi.org/10.1016/j.asej.2018.01.005.
[18] Trask RS, Williams HR, Bond IP. Self-healing polymer composites: mimicking nature to enhance performance. Bioinspiration Biomimetics 2007. doi: https://doi.org/10.1088/1748-3182/2/1/P01.
[19] White SR, Sottos NR, Geubelle PH, Moore JS, Kessler MR, Sriram SR. Autonomic healing of polymer composites. Nature 2001. doi: https://doi.org/10.1038/35057232.
[20] Ghosh B, Urban MW. Self-repairing oxetane-substituted chitosan polyurethane networks. Science (80-) 2009. doi: https://doi.org/10.1126/science.1167391.
[21] Dailey MMC, Silvia AW, McIntire PJ, Wilson GO, Moore JS, White SR. A self-healing biomaterial based on free-radical polymerization. J Biomed Mater Res - Part A 2014. doi: https://doi.org/10.1002/jbm.a.34975.
[22] Maleha AAAE-F. The use of Meteorological Data and Geographic Information Systems (GIS) in the Integrated Management of Soil and Water for Sustainable Agriculture in Toshka. Ain Shams University; 2018.
[23] Kim K, Jung JY, Han HS. Utilization of microalgae in aquaculture system: Biological wastewater treatment. Emerg Sci J 2019.
[24] Cordier C, Guyomard K, Stavrakakis C, Sauvade P, Coelho F, Moulin P. Culture of microalgae with ultrafiltered seawater: a feasibility study. SciMedicine J 2020.
[25] Li L, Shi W, Yu S. Research on forward osmosis membrane technology still needs improvement in water recovery and wastewater treatment. Water (Switzerland) 2020. doi: https://doi.org/10.3390/w12010107.
[26] Zohuriaan-Mehr MJ, Kabiri K. Superabsorbent polymer materials: a review. Iran Polym J (English Ed 2008.
[27] Sartore L, Pandini S, Baldi F, Bignotti F, Di Landro L. Biocomposites based on poly(lactic acid) and superabsorbent sodium polyacrylate. J Appl Polym Sci 2017. doi: https://doi.org/10.1002/app.45655.
[28] Kiatkamjornwong S. Superabsorbent polymers and superabsorbent polymer composites. ScienceAsia 2007. doi: https://doi.org/10.2306/scienceasia1513-1874.2007.33(s1).039.
[29] Farooqi ZH, Khan HU, Shah SM, Siddiq M. Stability of poly(N-isopropylacrylamide-co-acrylic acid) polymer microgels under various conditions of temperature, pH and salt concentration. Arab J Chem 2017. doi: https://doi.org/10.1016/j.arabjc.2013.07.031.
[30] Mei CC, Stiassnie M, Yue DK-P. Theory and applications of ocean surface waves Part 1: Linear aspects; 2005.
[31] Stachiw JD. Acrylic plastic as structural material for underwater vehicles. In: 2004 Int. Symp. Underw. Technol. UT'04 - Proc.; 2004. https://doi.org/10.1109/ut.2004.1405581.
[32] Kang Z, Ni W, Ma G, Xu X. A model test investigation on vortex-induced motions of a buoyancy can. Mar Struct 2017. doi: https://doi.org/10.1016/j.marstruc.2017.01.004.
[33] Akpan PU, Jones S, Eke MN, Yeung H. Modelling and transient simulation of water flow in pipelines using WANDA Transient software. Ain Shams Eng J 2017. doi: https://doi.org/10.1016/j.asej.2015.09.006.
[34] Taştan K. Critical submergence for a horizontal pipe intake. Ain Shams Eng J 2020. doi: https://doi.org/10.1016/j.asej.2020.02.010.
[35] Extrand CW. Drainage of liquid from a small circular hole in a vertical wall. J Adhes Sci Technol 2018. doi: https://doi.org/10.1080/01694243.2017.1400802.
[36] Theingi M, Tun KT, Aung NN. Preparation, characterization and optical property of LaFeO3 nanoparticles via sol-gel combustion method. SciMedicine J 2019.
[37] Mahon R, Balogun Y, Oluyemi G, Njuguna J. Swelling performance of sodium polyacrylate and poly(acrylamide-co-acrylic acid) potassium salt. SN Appl Sci 2020. doi: https://doi.org/10.1007/s42452-019-1874-5.
[38] Rashwan IMH, Idress MI. Brink as a device for measurement discharge for partially filled circular channel. Ain Shams Eng J 2013. doi: https://doi.org/10.1016/j.asej.2012.08.003.

Associate Professor Gang Ma is working in College of Shipbuilding Engineering, Harbin Engineering University. His research interests are renewable offshore energy engineering, dynamic of ocean engineering structures, nonlinearity of mooring lines, hydrodynamic, finite element analysis, and offshore platforms.

Muhammad Hanis Kamaruddin is a PhD candidate in College of Shipbuilding Engineering, Harbin Engineering University. Currently, his PhD studies is mainly in renewable offshore structures, focussing on floating offshore wind turbine structures and optimisation of mooring lines. His research interests are floating offshore renewable energy, nonlinear dynamics of offshore platforms, coupled analysis of offshore floating structure, and smart materials applications for ocean engineering.

Dr. Hooi-Siang Kang is the Director of the Marine Technology Centre at UTM. He has published over 60 international journal and conference papers. His research interests are the floating renewable energy system, microalgal aquaculture, and smart materials for ship and ocean engineering. He is an international advisory editorial board member for the Journal of Ocean Engineering and Technology by Korean Society of Ocean Engineers. Dr. Kang is actively involved in multiple international grants, including Erasmus+, Horizon 2020, Korean JTP in the area of engineering education and offshore engineering.

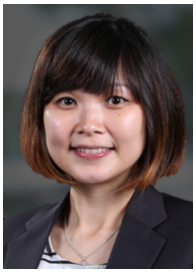

Dr. Pei Sean Goh is an associate professor the School of Chemical Engineering at the Universiti Teknologi Malaysia (UTM). Dr. Goh is a research fellow of the Advanced Membrane Research Technology Research Centre (AMTEC), UTM. She is also the Head of Nanostructured Materials Research Group in UTM. Her research interests focus on the synthesis of a wide range of nanostructured materials and their composites for membrane-based separation processes. Dr. Goh has authored or co-authored more than 100 research papers.

Professor Moo-Hyun Kim is a professor in the Department of Ocean Engineering, Texas A&M University. He has published over 250 international journal and conference papers. His research interests are nonlinear dynamics of offshore platforms, wave mechanics and free-surface flows, nonlinear stochastic analysis, computational fluid dynamics, hydroelasticity, floating breakwaters, beach erosion, multi-hull-riser-mooring coupled dynamic analysis, liquid-sloshing & vessel-motion interactions, ocean renewable energy (floating offshore wind turbine) & wave energy conversion), and smart offshore platforms.

Dr. Kee-Quen Lee is the head of acoustic lab in Malaysia-Japan International Institute of Technology, UTM. Her research interest is marine structural vibration, ocean renewable energy system, and moored structure dynamics. Currently she has research collaboration on marine related topic with researchers from Department of Naval Architecture and Ocean Engineering, Osaka University, Japan.

Dr. Cheng Yee Ng is current a senior lecturer in Department of Civil and Environmental Engineering, Universiti Teknologi PETRONAS (UTP), Malaysia. She received her BEng in Civil Engineering (2008), MSc in Civil Engineering (Offshore Structures) in 2010 and PhD in Civil Engineering (Offshore Structures) in 2014 from UTP. She returned to her alma mater UTP in year 2014 as a lecturer. In her current research, she's focusing on Engineering Education, Offshore Structures and Renewable Energy.